

Supporting information

Amorphous/Low-Crystalline Core/Shell Type Nanoparticles as a Highly Efficient and Self-Stabilizing Catalyst for Alkaline Hydrogen Evolution

Yanfang Wu,^a Ming Zhao,^{a,} Jing-Pei Cao,^a Jing Xu,^{b,*} Tienan Jin,^c and Naoki Asao^{d,*}*

^aKey Laboratory of Coal Processing and Efficient Utilization (Ministry of Education),
China University of Mining & Technology, Xuzhou 221116, P. R. China

^bCollege of Chemical Engineering and Materials Science, Quanzhou Normal
University, Quanzhou 362000, P. R. China

^cAdvanced Institute for Materials Research, Tohoku University, Sendai 980-8577, Japan

^dGraduate School of Science and Technology, Shinshu University, Ueda 386-8567,
Japan

E-mail: jingxu_1003@126.com; ming815zhao@163.com; asao@shinshu-u.ac.jp

1. Chemicals and materials. Palladium acetylacetonate ($\text{Pd}(\text{acac})_2$, 99%), nickel acetylacetonate ($\text{Ni}(\text{acac})_2$, 95%), platinum acetylacetonate ($\text{Pt}(\text{acac})_2$, 97%), triphenylphosphine (TPP, 99%), trioctylphosphine oxide (TOPO, technical grade, 90%), oleylamine (OAm, technical grade, 70%), tetra-n-butylammonium bromide (TBAB, 99%), and nafion perfluorinated ion-exchange resin (5 wt % solution in a lower aliphatic alcohol/ H_2O mixture that contains 15-20% water) were all purchased from Sigma-Aldrich. Commercial Pt/C (Johnson Matthey, 20 wt%) was purchased from Sunlrite Co. Ltd. Carbon black (Vulcan XC-72) was purchased from Moubic Inc. All the chemicals were used as received without further purification.

2. Material characterization. X-ray diffraction (XRD) patterns were recorded on a Rigaku RINT Ultima III instrument to study the crystallographic information of the samples. Transmission electron microscopy (TEM), high-resolution TEM (HRTEM), and selected area diffraction (SAED) were performed on a JEOL JEM-2100 (HR) instrument operated at 200 kV to analyze the morphology and crystallinity of the samples. The high-angle annular dark-field scanning transmission electron microscopy (HAADF-STEM) and elemental mappings were carried out by using JEOL JEM-ARM200F to confirm the nanostructure. Energy-dispersive X-ray spectroscopy (EDS) line scan was performed with a JEOL JED-2300T. The compositions of the samples were determined by inductively coupled plasma mass spectrometry (ICP-MS) using an Agilent 8800 instrument.

3. Experimental Section.

3.1 Catalyst preparation.

Synthesis of Pd-P/Ni NPs: 30.5 mg of $\text{Pd}(\text{acac})_2$ (0.1 mmol), 77 mg of $\text{Ni}(\text{acac})_2$ (0.3 mmol), 232 mg of TPP (0.88 mmol), 322 mg of TBAB (1 mmol), 1.16 g of TOPO (3 mmol), and 6.5 mL of OAm were mixed under a nitrogen flow at 50 °C for 25 min. The formed solution was heated to 220 °C at a constant heating rate of 12 °C min⁻¹ and kept at 220 °C for 30 min. Then, the mixture was cooled to room temperature, followed by

centrifugation at 10,000 rpm for 8 min and washed with ethanol. Finally, the Pd-P/Ni NPs were collected and dried at room temperature for 1 h.

Synthesis of Pd-P/Pt-Ni core-shell type NPs: The obtained Pd-P/Ni NPs were dispersed in 17 mL OAm and then 322 mg TBAB (1 mmol), 1.16 g of TOPO (3 mmol), 51.1 mg of Pt(acac)₂ (0.13 mmol) were added into the mixture, followed by deaerating (nitrogen gas) for 25 min at room temperature. The resulting solution was slowly heated to 200 °C in 50 min and kept at 200 °C for 30 min. After cooling to room temperature, the product was collected by centrifugation and washed with ethanol twice.

Synthesis of Pd-P/Pt-Ni/C and Pd-P/Pt-Ni/C-Ac: Vulcan XC-72 (112 mg) in hexane (230 mL) was sonicated for 30 min, and a suspension of Pd-P/Pt-Ni NPs in hexane (48 mg in 150 mL) was added. The resultant mixture was sonicated again for further 30 min to get the homogeneous solution. After evaporating the hexane, the remained solid material (i.e., Pd-P/Pt-Ni/C) was dispersed in acetic acid (100 mL) and heated at 70 °C under a nitrogen gas atmosphere for 12 h. The resulting material was separated by centrifugation, washed with ethanol three times, and dried to afford Pd-P/Pt-Ni/C-Ac.

3.2 Electrochemical measurements.

All the electrochemical experiments are performed on a CHI660 electrochemical analyzer supplied by CH Instruments Ins. A conventional three-electrode cell was used, including the Ag/AgCl (filled with saturated KCl) electrode as a reference electrode, a carbon rod as the counter electrode, and a modified L-shape glassy carbon electrode (with a surface area of 0.07 cm², BAS Inc.) as the working electrode. The potential value used in LSV profiles were changed from E(Ag/AgCl) to E(RHE), according to the formula $E(\text{RHE}) = E(\text{Ag/AgCl}) + 0.2224 \text{ volts} + 0.05916 \times \text{pH volts}$. For the electro-catalyst preparation, a mixture of catalyst (around 2.0 mg), nafion (10 μL), distilled H₂O (95 μL), and ethanol (95 μL) was ultrasonically dispersed for 20 min to form an ink. The modified GCE was coated with the as-obtained catalyst ink and dried naturally at room temperature. Linear sweep voltammetry (LSV) experiments are carried out in a N₂

saturated 1.0 M KOH aqueous solution at a scan rate of 10 mV s⁻¹ at 298 K with iR compensation (90%). The current density is normalized by the geometric area of the L-shape GC electrode.

4. Scherrer formula

Scherrer formula: $d = K\lambda/w\cos\theta$, where d is the particle size, λ is the wavelength of the radiation, θ is the angle of the considered Bragg reflection, w is the width on a 2θ scale, and K is a constant close to unity.

The (220) peak of Pd-P@Pt-Ni/C-Ac (Fig. 2f) was chosen to determine the crystallite size of Pt-Ni shell. According to Scherrer formula and the values of K , λ , θ , and w , the crystallite size which is also the approximate thickness of Pt-Ni shell was calculated to be 1.45 nm. The calculation details are shown below:

$$K = 0.89$$

$$\lambda = 0.154 \text{ nm}$$

$$2\theta = 68.5^\circ$$

$$w = 0.114 \text{ rad}$$

$$d \text{ (nm)} = \frac{0.89 \cdot 0.154}{0.114 \cdot \cos\left(\frac{68.5}{2}\right)} = 1.45 \text{ nm}$$

5. Turnover frequency (TOF)

The TOF values were calculated based on the following equation:

$$\text{TOF(/s)} = jS/2nF$$

F: the Faraday constant of 96,487 C/mol;

n: the mole number of Pt loaded on the working electrode;

S: the geometric area of the working electrode;

j: the current density at 100 mV (based on the LSV curves of HER).

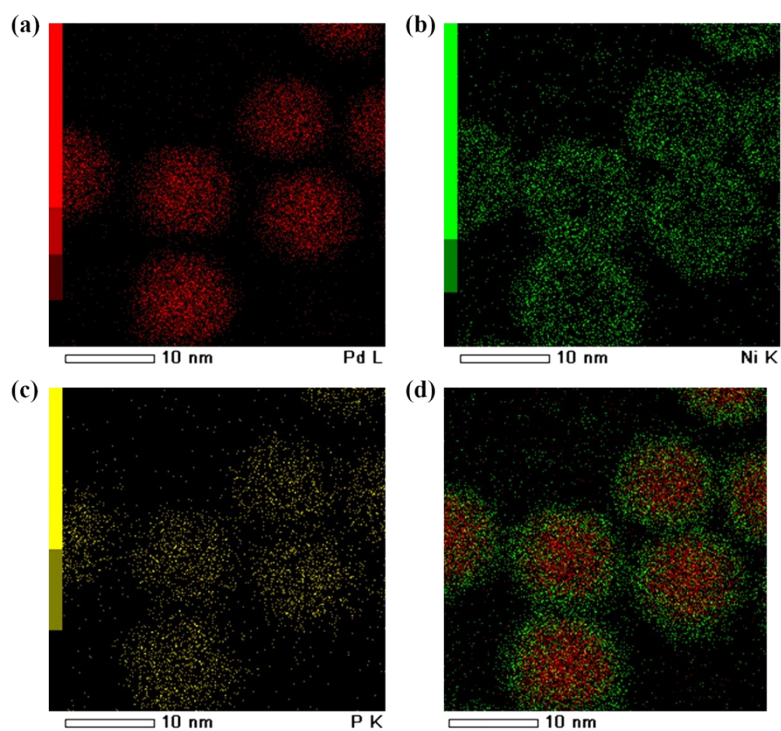


Figure S1. STEM elemental mappings of (a) Pd, (b) Ni, (c) P and (d) their overlap in Pd-P/Ni NPs.

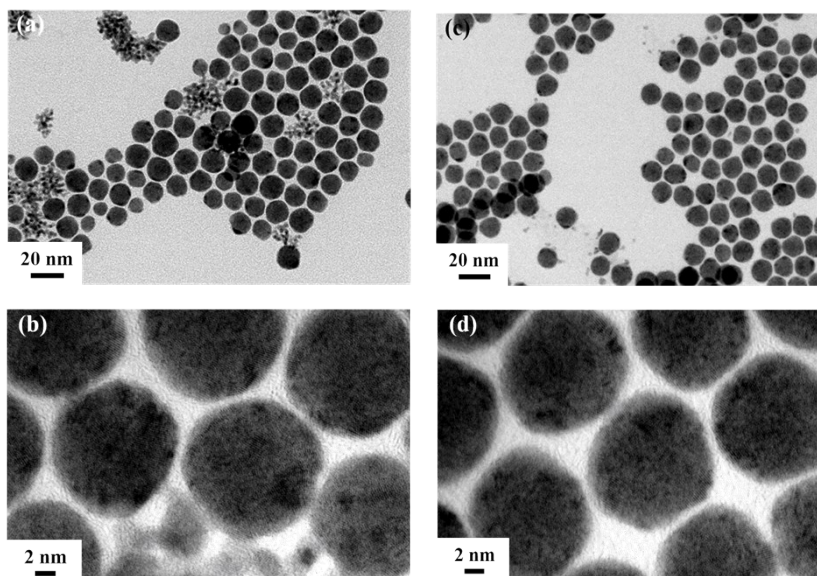


Figure S2. The synthesized Pd-P/Pt-Ni NPs with higher concentration of Pt(acac)₂. (a-b) Pt(acac)₂/OLA = 0.15 mmol/10 mL; (c-d) Pt(acac)₂/OLA = 0.1 mmol/10 mL.

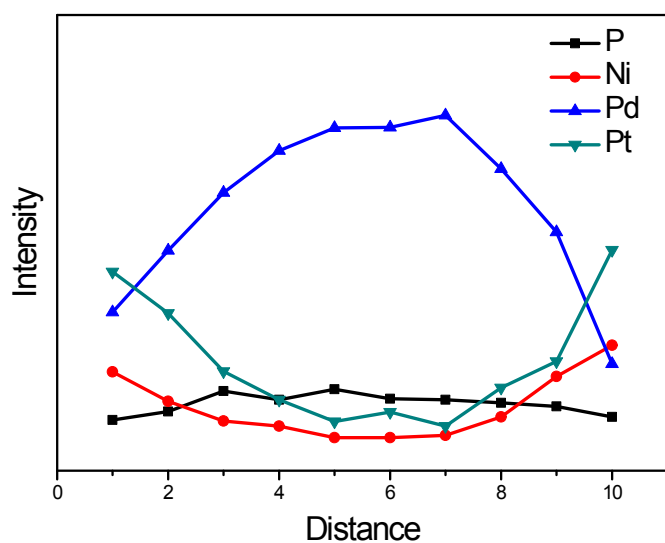


Figure S3. EDS line scan profiles across single Pd-P/Pt-Ni NP.

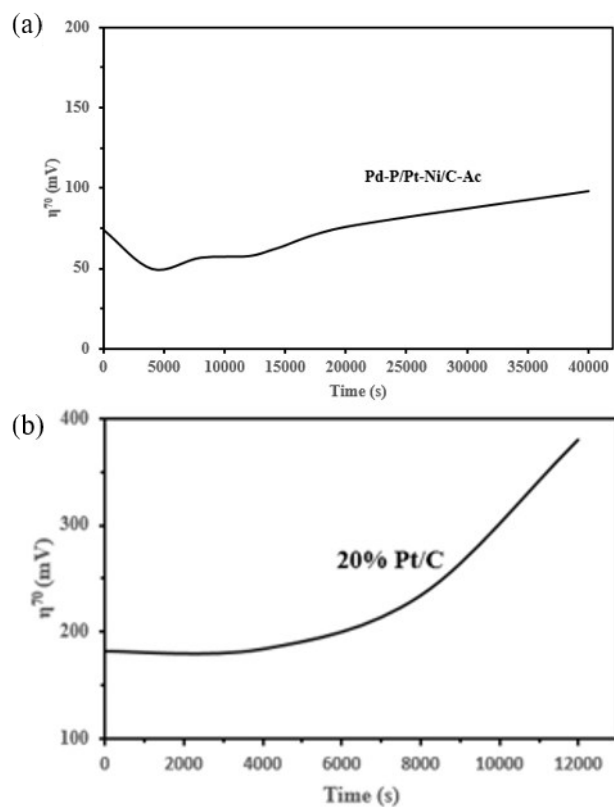


Figure S4. The changes on overpotentials with time by using Pd-P/Pt-Ni/-Ac (a) or Pt/C (b) as elector-catalysts in alkaline HER.

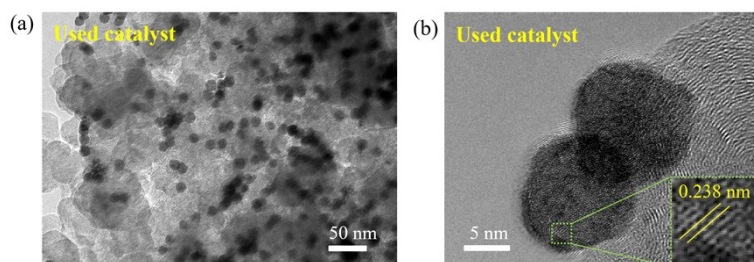


Figure S5. TEM (a) and HRTEM (b, with a magnified image as an inset showing the lattice spaces) images of Pd-P/Pt-Ni/C-Ac after the stability test.

6. References for Figure 3c.

1. Z. C. Zhang, G. G. Liu, X. Y. Cui, B. Chen, Y. H. Zhu, Y. Gong, F. Saleem, S. B. Xi, Y. H. Du, A. Borgna, Z. C. Lai, Q. H. Zhang, B. Li, Y. Zong, Y. Han, L. Gu and H. Zhang, *Adv. Mater.*, 2018, **30**, 1801741.
2. A. Alinezhad, L. Gloag, T. M. Benedetti, S. Cheong, R. F. Webster, M. Roelsgaard, B. B. Iversen, W. Schuhmann, J. J. Gooding and R. D. Tilley, *J. Am. Chem. Soc.*, 2019, **141**, 16202-16207.
3. M. M. Lao, K. Rui, G. Q. Zhao, P. X. Cui, X. S. Zheng, S. X. Dou and W. P. Sun, *Angew. Chem. Int. Ed.*, 2019, **58**, 5432-5437.
4. Y. F. Xie, J. Y. Cai, Y. S. Wu, Y. P. Zang, X. S. Zheng, J. Ye, P. X. Cui, S. W. Niu, Y. Liu, J. F. Zhu, X. J. Liu, G. M. Wang and Y. T. Qian, *Adv. Mater.*, 2019, **31**, 1807780.
5. W. C. Records, Y. Yoon, J. F. Ohmura, N. Chanut and A. M. Belcher, *Nano Energy*, 2019, **58**, 167-174.
6. Z. M. Cao, Q. L. Chen, J. W. Zhang, H. Q. Li, Y. Q. Jiang, S. Y. Shen, G. Fu, B. A. Lu, Z. X. Xie and L. S. Zheng, *Nat. Commun.*, 2017, **8**, 15131.
7. R. Kaviani, S. I. Choi, J. Park, T. Y. Liu, H. C. Peng, N. Lu, J. G. Wang, M. J. Kim, Y. N. Xia and S. W. Lee, *J. Mater. Chem. A*, 2016, **4**, 12392-12397.
8. P. T. Wang, K. Z. Jiang, G. M. Wang, J. L. Yao and X. Q. Huang, *Angew. Chem. Int. Ed.*, 2016, **55**, 12859-12863.
9. L. S. Xie, X. Ren, Q. Liu, G. W. Cui, R. X. Ge, A. M. Asiri, X. P. Sun, Q. J. Zhang and L. Chen, *J. Mater. Chem. A*, 2018, **6**, 1967-1970.
10. L. Wang, C. Lin, D. K. Huang, J. M. Chen, L. Jiang, M. K. Wang, L. F. Chi, L. Shi and J. Jin, *ACS Catal.*, 2015, **5**, 3801-3806.

11. Z. K. Du, Y. L. Wang, J. S. Li and J. P. Liu, *J. Nanopart. Res.*, 2019, **21**, 13.
12. M. Nadeem, G. Yasin, M. H. Bhatti, M. Mehmood, M. Arif and L. M. Dai, *J. Power Sources*, 2018, **402**, 34-42.
13. Z. Zhao, H. Liu, W. Gao, W. Xue, Z. Liu, J. Huang, X. Pan and Y. Huang, *J. Am. Chem. Soc.*, 2018, **140**, 9046-9050.
14. Z. M. Cao, H. Q. Li, C. Y. Zhan, J. W. Zhang, W. Wang, B. B. Xu, F. Lu, Y. Q. Jiang, Z. X. Xie and L. S. Zheng, *Nanoscale*, 2018, **10**, 5072-5077.